

T113  
Y12  
3570

YALE MEDICAL LIBRARY



3 9002 08676 3076

**DUAL RADIONUCLIDE STUDY OF  
MYOCARDIAL INFARCTION:**

RELATIONSHIPS BETWEEN  
MYOCARDIAL UPTAKE OF POTASSIUM-43,  
TECHNETIUM-99M STANNOUS PYROPHOSPHATE,  
AND REGIONAL MYOCARDIAL BLOOD FLOW



**VINCENT CHARLES DICOLA**

**1976**



YALE



MEDICAL LIBRARY

YALE



MEDICAL LIBRARY



Digitized by the Internet Archive  
in 2017 with funding from  
Arcadia Fund

<https://archive.org/details/dualradionuclide00dico>







DUAL RADIONUCLIDE STUDY OF MYOCARDIAL INFARCTION:  
RELATIONSHIPS BETWEEN MYOCARDIAL UPTAKE OF  
POTASSIUM-43, TECHNETIUM-99M STANNOUS PYROPHOSPHATE,  
AND REGIONAL MYOCARDIAL BLOOD FLOW

VINCENT CHARLES DICOLA  
B.A., BROWN UNIVERSITY, 1972

A THESIS SUBMITTED IN PARTIAL FULFILLMENT  
OF THE REQUIREMENTS FOR THE DEGREE OF  
DOCTOR OF MEDICINE  
YALE UNIVERSITY SCHOOL OF MEDICINE

1976





Permission for photocopying or microfilming of "

Dual Radionuclide

Study of Myocardial Infarction

(TITLE OF THESIS)

for the purpose of individual scholarly consultation or reference is hereby granted by the author. This permission is not to be interpreted as affecting publication of this work or otherwise placing it in the public domain, and the author reserves all rights of ownership guaranteed under common law protection of unpublished manuscripts.

Vincent Charles DiCola

Signature of Author

April 12, 1976

Date



DEDICATED TO  
MY MOTHER AND FATHER  
WITH ALL MY LOVE



## ACKNOWLEDGEMENTS

Barry L. Zaret, M.D.

To acknowledge the excellent guidance and inspiration Dr. Zaret has given me in the study of both radionuclide imaging and clinical cardiology, I can only quote from Sir Issac Newton:

"If I have seen further, it is by standing on the shoulders of giants."

Robert C. Lange, Ph.D.

For many invaluable suggestions.

Mario Addabbo, M.S.

My friend, whose good cheer and quick hands helped save many an experiment.

Linda Bernstein

For amiable assistance and patient instruction.

My family

For their confidence, support, and sacrifices on my behalf.





## TABLE OF CONTENTS

Introduction.....	1
Microsphere Determinations of Regional Myocardial Blood Flow.....	4
Potassium-43.....	9
Technetium-99m Stannous Pyrophosphate.....	15
Materials and Methods.....	21
I. Radionuclides.....	21
II. Animal Protocol.....	21
Results.....	26
Discussion.....	29
Summary.....	34
Figures.....	36
Bibliography.....	43



## INTRODUCTION

Over the past decade the mortality from myocardial infarctions has been reduced significantly by the close monitoring and rapid treatment of its arrhythmic complications. With the development of new medical and surgical techniques designed to salvage ischemic myocardium, the knowledge of the site and size of a myocardial infarction has assumed greater therapeutic importance. This last point is most significant since the location, extent, and degree of associated ventricular dysfunction are major determinants governing the hemodynamic consequences and thus, the clinical course of a myocardial infarction.

Serum creatine phosphokinase enzyme determinations (1-3) and precordial ST segment mapping (4-6) are two relatively new, non-invasive methods for assessing the degree of myocardial damage. In addition, they have been used to gauge the effectiveness of certain drug and mechanical interventions designed to limit the amount of myocardial necrosis. It is well recognized, however, that precise electrocardiographic documentation of myocardial infarction is difficult if not impossible in some situations of previous myocardial infarction, of subendocardial infarction, and of left bundle branch block or other conduction delay. In addition, the specificity of cardiac enzyme abnormalities can be compromised by concomitant congestive heart failure, hemolysis, brain or



pulmonary damage, or intramuscular injections. Presently, the technique of radionuclide myocardial imaging holds promise as an alternative means of accurate qualitative and quantitative evaluation of ischemic and infarcted myocardium.

Non-invasive radionuclide imaging can visualize the region of ischemia and/or infarction in two general ways. On the one hand, radioisotopes of an intracellular cation such as potassium (K) or its analogues, Rubidium (Rb) Cesium (Cs), and Thallium (Tl), accumulate maximally in normal myocardium and minimally in ischemic tissue (7-14). Myocardial imaging of such a distribution would reveal the zone of infarction or ischemia as an area of relatively decreased radioactive tracer accumulation or "cold spot." Qualitatively, it cannot differentiate new from old areas of infarction but can be used to define transiently ischemic tissue.

Alternatively, other radionuclides such as technetium-99m labeled stannous pyrophosphate, tetracycline, or glucoheptonate and radioactively labelled myosin specific antibody, have a strong affinity for and maximally concentrate in recently infarcted myocardium (15-24). Imaging reveals the region of infarction as a zone of increased radionuclide accumulation or "hot spot." Although hot spot tracers are specific for recent infarctions, it is unclear whether they accumulate solely in necrotic cells or in reversibly damaged tissue as well.

By using both types of scanning agents simultaneously in the acute infarction period, one may be able to define





precisely the region of infarction and more importantly, an area of periinfarction ischemia. In fact, several recent reports suggest that the information obtained by scans with both types of agents is complementary and improves their overall accuracy (15, 25, 26). Furthermore, initial trials with both types of imaging agents have been used successfully to quantify the amount of abnormal ventricular myocardium present. Thus, serial evaluations of a myocardial infarction by dual radionuclide imaging may be useful for the assessment of therapeutic interventions during the course of a myocardial infarction.

Before it is appropriate to utilize this approach to quantify gradations of abnormality within the infarcted left ventricle, it is necessary to define accurately the pathophysiologic correlates of myocardial radionuclide uptake. With this purpose the myocardial distributions of potassium-43 ( $^{43}\text{K}$ ) and technetium-99m stannous pyrophosphate ( $^{99\text{m}}\text{Tc-PYP}$ ) were studied simultaneously in a canine model of acute myocardial infarction. Their interrelationships were evaluated and their regional uptake compared to regional myocardial blood flow, as measured by the radioactive microsphere technique. A review of the theoretical and experimental characteristics of microsphere estimates of regional myocardial blood flow and of the dual radionuclides  $^{43}\text{K}$  and  $^{99\text{m}}\text{Tc-PYP}$  will be followed by a presentation of the experimental data and a discussion of the implications of this study.



## MICROSPHERE DETERMINATIONS OF REGIONAL MYOCARDIAL BLOOD FLOW

Blood flow to the whole heart or to specific regions of it is a desirable and valuable measurement for both research and clinical evaluations (27). It would allow one to assess and define the physiological basis for critical coronary stenosis in experimental animals and in the clinical evaluation of patients with coronary artery disease (28). In addition, it would enable one to assess collateral blood flow and therapeutic manipulations of coronary blood flow (29-31). Finally, one could use it as a reference standard in the experimental evaluation of indirect and/or non-invasive methods of determining regional myocardial perfusion (32).

The determination of coronary blood flow, however, is difficult to measure experimentally. Electromagnetic or ultrasonic flowmeters or indicator dilution techniques are applicable for total flow but are difficult to perform for technical reasons. In addition, none of these can measure flow to a ventricle or any specific portion of it. Other methods, nitrous oxide washout (33), washout of indicators injected into the myocardium (34) or the coronary arteries (35), and isotope clearance techniques (36), either measure flow per unit weight of myocardium without referring to a specific region of the heart or are technically unsatisfactory because of the necessity of intracoronary injections.

In 1967 Rudolph and Heymann reported a method of measuring cardiac output to various organs by injecting carbonized microspheres labeled with gamma emitting nuclides (37). In principle, if the microspheres are well mixed prior



to ejection, are distributed according to blood flow, do not escape from the organs and do not disturb the circulation, then their fractional distribution will be proportional to the fraction of cardiac output going to those organs. Thus, if the flow to any organ is known, flow to another organ can be determined. In addition, since the microspheres are trapped in the precapillary vessels in their first transit, the radioactivity of any region within an organ is proportional to blood flow to that region.

Domenech et al. and Fortuin et al. proved that these assumptions held for the heart and that one could determine coronary blood flow (38, 39). More importantly, however, both groups showed that one could assess regional myocardial blood flow with microspheres. For example, using several different size microspheres they found that the left ventricle received approximately one and one half times the flow of the right ventricle, presumably because the increased energy requirements of the left ventricle necessitates higher blood flow. Similarly, they reported that the endocardial half of the ventricular wall receives more flow than the epicardial half. This measurement, however, varied with the size of the microsphere used, and one of the limitations of the microsphere technique became obvious. With large microspheres (50 microns) the endocardial to epicardial radioactivity ratio was 1.45 versus 1.12 for 15 micron microspheres. Other techniques reported values slightly above 1 (40,41). The falsely high value with large microspheres can be accounted for in two ways.





The large spheres would tend to stay in the center of blood flow and follow the perforating vessels to the endocardium. On the other hand, the smaller 15 micron spheres travel more peripherally like a red blood cell, have less tendency toward axial streaming, and distribute more easily to the epicardium. In addition, the 50 micron spheres may become trapped in the subendocardial plexus which fills with blood during diastole and then empties during systole because of high intramyocardial tension. Thus, the 15 micron spheres would more accurately estimate actual myocardial blood flow while the larger microspheres reflect flow during diastole alone. Smaller spheres also have several other advantages over larger ones. They are distributed more like red blood cells, occlude less of the vascular bed, are less variable in size, and most importantly can be given safely in greater amounts, thus allowing more reliable measurements of flow to small regions.

Buckberg et al. not only confirmed the validity of using microsphere techniques for measuring coronary blood flow, but also evaluated the sources of error inherent in this technique (42). Their results showed that differences in blood flow determinations are generally the result of random variation, i.e. poor mixing of the microspheres. These errors, however, could be minimized as long as each sample contained at least 400 microspheres. Furthermore, while smaller numbers of microspheres will be associated with larger random errors and a low precision of estimate, they would not systematically over-or underestimate mean flow. More



experiments, however, would be needed to demonstrate the significance of any given difference. Thus, the greatest precision occurs with the injection of the largest number of microspheres consistent with no physiological changes. Fortuin et al. showed that the reactivity of the coronary vascular bed, manifested by the ability to increase flow after a hyperemic stimulus such as transient coronary occlusion, was not diminished significantly by as many as  $12 \times 10^6$  15 micron microspheres (39).

Having observed these caveats, other experimenters reported important findings about regional myocardial blood flow that were especially pertinent to the endocardium since its blood flow is almost entirely diastolic and thus more prone to ischemia (43). In dogs with normal coronary arteries, Fortuin et al. showed endocardial blood flow was increased by propranolol, decreased by isoproterenol, and unchanged by nitroglycerin (39). In dogs with acute occlusions, Domenech found a radial gradient of flow with increasing flow from the center of the infarct outward (44). In a similar experiment, Becker et al. reported not only the same radial gradient of flow, but also that there was an inordinate reduction of flow to the endocardial half of the left ventricular wall (45). Other reports by Moir (46) and by Becker et al. (30) demonstrated that one could alter this disproportionate endocardial flow reduction in the ischemic area with nitroglycerin or propranolol.

Recent experiments using epicardial electrode maps and microsphere estimates of blood flow (31), showed that



while the beta adrenergic blocker, propranolol, decreased blood flow to the ischemic area, ST segment elevation also decreased. Similarly, isoproterenol increased blood flow and ST segment elevation. While they conclude that beta adrenergic agents do not alter ischemia through primary changes in blood flow distribution, it is well known that epicardial electrodes are insensitive to endocardial events.

Other experimenters have used microsphere estimates of blood flow to evaluate the perfusion estimates obtained with radioactive nuclides. Prokop et al. compared potassium-43 to labeled microspheres in terms of their ability to reflect alterations in regional myocardial blood flow (32). They found excellent correlation under conditions of normal and decreased flow although  $^{43}\text{K}$  was slightly less reduced at very low flows. Endocardial to epicardial flow ratios also agreed very well. At higher than normal flows, however,  $^{43}\text{K}$  estimate did not increase to the same extent as microspheres flow determinations. In similar experiments Becker et al. and Strauss et al. respectively compared Rubidium-86 and Thallium-201 estimates of regional myocardial perfusion to that obtained with microspheres (47,48). They also demonstrated excellent correlation except at very reduced flows or in cases of reactive hyperemia.

In conclusion, microspheres are accurate indicators of regional myocardial blood flow. They thus can be used as a reference standard to evaluate drug as well as other manipulations of coronary blood flow, and to evaluate the relation-





ship of flow to the myocardial uptake of other materials or to other parameters of cardiac function such as ST segment mapping.

### POTASSIUM-43

Potassium, one of the key intracellular cations, plays an important role in cellular metabolism. Cellular efflux of potassium, as evidenced by increased potassium ion in coronary sinus blood after atrial pacing, can be indicative of myocardial cell ischemia (49). Thus, differences in both intra- and extracellular potassium concentrations can reflect pathologic changes in the myocardium. Studies of potassium kinetics in the normal and diseased heart, therefore, were undertaken first with potassium-42 and then with potassium-43 in the hope that these radioactive isotopes could be useful in identifying ischemic myocardium.

Myocardial accumulation of radioactive potassium was first reported in 1941 with  $^{42}\text{K}$  (50). This work was not pursued, however, until 1954 when Love et al. reported similar myocardial uptake of both  $^{86}\text{Rb}$  and  $^{42}\text{K}$  (51). Accumulation in the myocardium was secondary to both regional myocardial blood flow and cellular uptake of the radioactive cation. In 1955 Conn and Robertson studied the kinetics of this transfer in the canine left ventricle (52), and by 1958 Sapirstein had shown that one could calculate myocardial blood flow by using the fractional uptake of potassium-42 by that organ (53).



An important development came in 1964, however, when Donato et al. showed that one could accurately quantitate the myocardial clearance of  $^{42}\text{K}$  and  $^{86}\text{Rb}$  by precordial counting after intravenous injection of the tracers (54). Their calculation of myocardial clearance of potassium agreed with estimates of myocardial blood flow obtained by the indirect Fick method and furthermore, showed that every unit of myocardium contributes to precordial counting rate. Thus, they showed that external counting of radionuclides could be correlated to myocardial perfusion.

Trials with  $^{42}\text{K}$  as a cold spot indicator of reduced coronary perfusion were also attempted. In animals with experimentally induced coronary stenosis Love et al. located the area of reduced perfusion with  $^{42}\text{K}$  scans (55). Bennett et al. showed that there was good correlation between poorly perfused areas on  $^{42}\text{K}$  scans and stenosis of coronary arteries supplying these areas (56). During this same period other investigators were also experimenting with analogues of potassium such as cesium and rubidium, as "cold spot" indicators of infarction, and there were several reports of successful detection of myocardial infarction (57, 58). These isotopes of rubidium ( $^{86}\text{Rb}$ ) and Cesium ( $^{131}\text{Cs}$ ) have not been completely satisfactory, however, because their gamma ray and other emissions have not been suitable for detection by conventional imaging instruments in doses permissible in man.  $^{42}\text{K}$  also emits a high energy proton which makes detection and imaging of the myocardium difficult.

In 1971, however, a new radioisotope of potassium,  $^{43}\text{K}$ ,



was reported by Hurley et al. to be useful in imaging acute myocardial infarction, and many of the advances in cold spot imaging in the clinical setting have been done using this isotope (59). They showed that  $^{43}\text{K}$  localized predominantly in the left ventricular and septal muscle. As with other isotopes mentioned, the thinner right ventricle and atria were less well defined and areas of infarction were seen as "cold spots." In clinical trials with  $^{43}\text{K}$ , 19 of 20 patients with myocardial infarction had excellent correlation of electrocardiographic, enzyme, arteriographic, and ventriculographic data with abnormalities on  $^{43}\text{K}$  perfusion scan (60).

Zaret and others extended the use of  $^{43}\text{K}$  perfusion scans to the study of ischemic as well as infarcted myocardium by evaluating patients both at rest and during maximal treadmill exercise (7). In the resting state, non-infarcted myocardium supplied by stenotic major coronary arteries are probably adequately perfused either through the stenotic vessel itself or through collaterals. With exercise, however, these areas are subject to inadequate perfusion. In 12 normal subjects  $^{43}\text{K}$  distribution was homogenous both at rest and during exercise. In 13 of 15 patients with previous myocardial infarction studied at rest, regions of decreased radionuclide accumulation corresponded to the anatomic location of the infarct. In 16 of 19 patients with angina pectoris clinically, regions of decreased  $^{43}\text{K}$  accumulation were present when the tracer was given during exercise but not at rest. Furthermore, these zones of relative hypoperfusion corresponded to regions supplied by angiographically



proven stenotic coronary arteries.

$^{43}\text{K}$  scans also were used to study false positive electrocardiographic exercise tests. These patients had normal coronary arteriography, left ventriculography and hemodynamic evaluation. All nine patients who were exercised to the point of abnormal ECG changes and then given  $^{43}\text{K}$  intravenously showed a homogenous distribution of isotope. This is in contrast to patients with coronary artery disease who show abnormal regions on  $^{43}\text{K}$  scan during exercise-induced ischemia (61).

Patients undergoing surgery for myocardial revascularization, also were studied both pre-and post-operatively and showed definite improvement in perfusion with the  $^{43}\text{K}$  scan 6 to 14 days after surgery (62). Zaret et al. demonstrated the value of the  $^{43}\text{K}$  scan in assessing the results of coronary bypass surgery (63). Scans which showed improved or normal uptake correlated well with 13 of 16 patent grafts seen on postoperative angiography. Scans which had not improved or worsened correlated with patients who had experienced intraoperative infarction, those with significant distal coronary artery disease, and those with occluded grafts. Finally, computer analysis of serial  $^{43}\text{K}$  scans in patients undergoing revascularization surgery demonstrated higher uptake after surgery (64).

Finally, Zaret et al. used  $^{43}\text{K}$  to semi-quantify myocardial infarctions (9). In 15 consecutive post MI patients who underwent angiographic evaluations, the total





area of  $^{43}\text{K}$  hypoperfusion on myocardial scanning correlated very highly with the total area of abnormally contracting segments of the left ventricle by angiography. Thus,  $^{43}\text{K}$  is useful for not only qualitative evaluation of the myocardium but also for quantification of the amount of abnormal tissue present in the left ventricle.

The diagnostic accuracy of  $^{43}\text{K}$  scans was compared to clinical, laboratory, electrocardiographic, and catheterization data in 85 patients (65). While two cardiologists interpreted all information except the  $^{43}\text{K}$  scan, nuclear medicine specialists interpreted only the scan. The significantly high agreement between the two modes of investigation was as follows: in previous myocardial infarction 88% agreement; in acute infarction 94%; in patients with coronary artery disease but without infarction 89% agreement. Thus,  $^{43}\text{K}$  is useful in the qualitative and quantitative evaluation of myocardial ischemia.

The physical characteristics of potassium-43, however, do present drawbacks for routine clinical use (66,67). Since it is produced from a cyclotron and has a very short half life, its costs and availability limit widespread applicability. Furthermore, while the total body dose of radiation is very low (0.81 rads per millicurie), its high emission energies (peaks of 590-610 and 370-390 KeV) make imaging difficult.  $^{43}\text{K}$  was used in this study, however, not only because of this laboratory's extensive use and familiarity with this tracer, but also because the mechanism in which the myocardium handles "cold spot" monovalent cations is generally similar. Thus,



statements about the uptake of  $^{43}\text{K}$  and its relationship to the distribution of hot spot agents would generally hold for newer agents such as Thallium-201 and Rubidium-81.



## TECHNETIUM-99m STANNOUS PYROPHOSPHATE

The use of a positive infarct-imaging agent was first reported in 1962 by Carr et al. who described the use of  $^{203}\text{Hg}$ -Chlormerodrin for photoscanning experimental myocardial infarctions in dogs (68). Since 1970 work in this area has increased exponentially and many radiopharmaceuticals which are sequestered by acutely infarcted tissue have been developed. Among these are the mercurials,  $^{203}\text{Hg}$ -Chlormerodrin (68) and  $^{203}\text{Hg}$ -Mercurifluorescein (69), gallium-67 citrate (70), and technetium-99m-labelled tetracycline (18), glucoheptonate (19-22), and pyrophosphate (15-17), and radioactively labeled myosin specific antibody (23-24).

The early work done with these compounds pointed out not only their shortcomings but also some of the ideal qualities necessary for a positive scanning agent. Although initial trials with a number of different mercurial compounds were promising in animal infarctions, attempts to extend this work to man were uniformly unsuccessful (68,69). The major cause for failure may have been the low radioactivity ratios between normal and diseased tissue which prevented good resolution infarct scanning, although inadequate amount of tracer and other technical difficulties were contributory. In addition, the high dose of radiation to the kidneys and long half life of  $^{203}\text{Hg}$  (45 days) were distinct drawbacks for human use.



In 1973 Kramer et al. reported that gallium-67 citrate, a radiopharmaceutical which accumulates in inflammatory and neoplastic tissue, also concentrates significantly in regions of experimental canine infarction (70). Concentrations in adjacent structures, however, caused great difficulty in interpretation of the gallium myocardial scan and have limited its applicability.

Similarly, Malek et al. demonstrated in 1963 that tetracycline accumulated around an area of myocardial infarction (71). By combining the excellent physical characteristics of  $^{99m}\text{Tc}$  with tetracycline and applying  $^{99m}\text{Tc}$ -tetracycline to the myocardium, Holman et al. not only demonstrated that "hot spot" infarct scanning could detect and size an acute myocardial infarction but also made a major advance toward developing the ideal hot spot agent (18).  $^{99m}\text{Tc}$ -tetracycline does have drawbacks however. First of all, it labels the liver so that diaphragmatic or inferior myocardial infarctions are difficult to visualize. Further, one must wait twenty-four hours after infarction before intravenous technetium-99m tetracycline will begin to accumulate in infarcted tissue; then one must wait an additional twenty-four hours before it is adequately concentrated to give meaningful images.

The bone scanning agent technetium-99m pyrophosphate ( $^{99m}\text{Tc}$ -PYP) has overcome these problems of safety, inadequate or slow uptake, and interference from surrounding tissue accumulation and has proven to be the most successful agent for myocardial scintograms yet developed. A recent comparative





study, in fact, showed the superiority of  $^{99m}\text{Tc}$ -PYP over technetium-99m labeled tetracycline and glucoheptonate in detecting myocardial infarction (22).

Bonte et al. first demonstrated that  $^{99m}\text{Tc}$ -PYP scintograms are positive in dogs with experimental myocardial infarction (16). These abnormal scintograms begin as early as twelve hours after infarction and from 45-60 minutes after intravenous injection of the isotope and remain unchanged for approximately six days. Thereafter they begin to fade, ordinarily becoming negative by the 14th post-infarction day. Similarly, in 202 patients admitted with chest pain of uncertain etiology, Willerson et al. demonstrated that there was almost precise correlation between the ECG and  $^{99m}\text{Tc}$ -PYP localization of the site of acute transmural infarctions (17). The time course of positive scintograms was similar to that shown in dogs. Of the 101 patients with clinical and laboratory confirmed myocardial infarction only five had negative scans and these were all performed seven or more days after infarction. Furthermore, because of its short half life, repeat  $^{99m}\text{Tc}$ -PYP scans could be obtained at 24 hour intervals for sequential evaluation. Of the 101 patients without confirmed infarction only nine had a positive scan and significantly, seven of these had a clinical diagnosis of "unstable angina pectoris." Klein et al. also showed that  $^{99m}\text{Tc}$ -PYP scans were highly sensitive indicators of infarction when compared to creatine phosphokinase (CPK) isoenzyme determinations (72). In addition they stated that isoenzymes and  $^{99m}\text{Tc}$ -PYP scintigrams are concordant after graded ischemia



in dogs.

Furthermore, the difficult diagnosis of subendocardial myocardial infarction could be made with  $^{99m}\text{Tc}$ -PYP scintograms (73). Recent reports, however, do suggest that the accuracy of  $^{99m}\text{Tc}$ -PYP scans can be improved by concomitant imaging with a cold spot agent especially in cases of subendocardial infarctions (25, 26).

Although the ability of  $^{99m}\text{Tc}$ -PYP to define precisely an area of myocardial infarction or ischemia has been clearly demonstrated, information regarding its ability to quantitate the size of infarction remains incomplete. In preliminary studies by Shames et al. (74), Willerson et al. (75), and Botvinick et al. (76), there was excellent correlation between size of infarction as determined by scintograms and by pathologic analysis. In humans, Willerson et al. showed good correlation between total serum CPK and  $^{99m}\text{Tc}$ -PYP myocardial scintogram determinations of infarct size in anterior but not in inferior or subendocardial myocardial infarctions. Further work is in progress and centers around the use of both a hot spot and a cold spot indicator of infarction to better define the area of damage. Initial reports by Poe et al. using Cesium-129 and  $^{99m}\text{Tc}$ -PYP and either  $^{43}\text{K}$  or  $^{201}\text{Tl}$  showed that valuable additional information was gained about the site and size of infarction (15,25,26).

Quantification with  $^{99m}\text{Tc}$ -PYP, however, will also depend on better understanding of the difficult and controversial questions regarding its mechanism of cellular uptake



and localization. In bone scanning  $^{99m}\text{Tc}$ -PYP, an anionic chelator, is most likely bound to the bone cations, chiefly calcium. In 1964 D'Agostino noted that calcium localized in the mitochondria of myocardial cells in steroid-induced focal necrosis (78). Furthermore, he and Chiga noted that it seemed to be bound in a crystalline structure which they believed to be hydroxyapatite (79). Finally, Shen and Jennings described similar calcium accumulation as an index of irreversible ischemic myocardial cell damage (89). These observations thus led Bonte et al. to their initial animal infarction experiments mentioned above.

Further morphologic work on this problem by Buja et al. has been interpreted as supporting the idea of  $^{99m}\text{Tc}$ -PYP as a hydroxapatite labeling agent (81,82). In some dogs with experimental myocardial infarction, positive myocardial scintograms showed a "doughnut" pattern, characterized by marked peripheral concentration of radioactivity around central zones of much lower activity and this was confirmed by relative tissue radioactivity counts. When these tissues were examined histologically, there was selective occurrence in the peripheral zones of calcified muscle cells with ultra-structurally demonstrable apatite-like crystals in the mitochondria. Buja et al. interpreted this as presumptive evidence favoring a temporal and topographical relationship between calcium accumulation and  $^{99m}\text{Tc}$ -PYP uptake in acute myocardial infarcts. They also admitted, however, that  $^{99m}\text{Tc}$ -PYP uptake may have resulted from accumulation in regions of residual perfusion into which the agent could



gain access. This point is bolstered by the reports of Poe et al. who showed that high  $^{99m}\text{Tc}$ -PYP were often found with good  $^{43}\text{K}$  concentrations and concluded that some perfusion is necessary for positive  $^{99m}\text{Tc}$ -PYP uptake (82). Furthermore, other localization studies notably by Dewanjee et al. seem to indicate that apatite formation is not directly responsible for localization of  $^{99m}\text{Tc}$  chelate (84). By differential centrifugation studies Dewanjee et al. showed that 50% of the radioactivity is in the lysosomal enzyme fraction of the cell while only 10-20% is in the mitochondrial fraction. The mitochondria, however, are the subcellular site of calcium localization following infarction. Thus, the biochemical mechanisms governing  $^{99m}\text{Tc}$ -PYP uptake have not been resolved.

At the present time, then,  $^{99m}\text{Tc}$ -PYP has been shown to be a safe (85) and sensitive method of detecting myocardial infarcts as early as 12 hours after their development. It has also proven useful in quantifying the extent of myocardial damage. While newer agents such as  $^{99m}\text{Tc}$ -glucoheptonate and radioactively labeled myosin specific antibody accumulate earlier in the course of a myocardial infarction, much experimental work must be done before any hot spot substance will be proven as efficacious as  $^{99m}\text{Tc}$ -PYP (22-24).





## MATERIALS AND METHODS

### I RADIONUCLIDES

The microspheres used in this study were supplied by the Nuclear Products Division of Minnesota Mining and Manufacturing Company. They had an average diameter of  $15 \pm 5$  microns and were labeled with Chromium-51, an isotope with principle peak gamma radiation of 320 KeV and a half life of 27.8 days. They were suspended in 10% dextran, had a specific activity of 10.8 millicuries (mCi) per gram, and a concentration of  $4.4 \times 10^6$  spheres per milliliter (ml).

Potassium-43 was obtained as a cyclotron-produced, sterile, pyrogen-free radionuclide in 0.9% normal saline from Oak Ridge National Laboratories, Oak Ridge, Tennessee. Its composition at calibration time was  $^{43}\text{K}$ -1mCi/ml  $\pm 0.2$  mCi/ml and it contained less than 5%  $^{42}\text{K}$ . Its peak energies are at 590-610 and 370-390 KeV and it has a 22.4 hour physical half-life.

The technetium-99m stannous pyrophosphate was obtained commercially from Mallinckrodt Chemical Works. Technetium-99m has a peak energy of 140 KeV and a physical half-life of 6.8 hours.

### II ANIMAL PROTOCOL

Adult mongrel dogs of either sex weighing between 20 and 35 Kg were used for all studies. A closed-chest myocardial infarction was created by modification of the catheter plug embolization technique of Cohen and Eldh as



follows (86). Animals were lightly anesthetized with intravenous sodium pentobarbital (30 mg/kg) and then intubated. The neck and anterior and lateral thorax were shaved. After a right jugular venous cutdown for fluid and medication administration was performed, a number 7 Sones catheter was introduced into the aortic root via the right carotid artery. After subselective positioning of the catheter into the left anterior descending coronary artery under fluoroscopic control, a guidewire-impaled plug present at the catheter tip was dislodged into the coronary circulation. This plug was 2-4mm long and made from the solid tip of a polyethylene angiographic catheter; it would generally lodge in the distal one third of the coronary circulation at the origin of the last large diagonal branch of the anterior descending. Animals were placed on a Harvard respirator and were pretreated with a 100mg-bolus of xylocaine just prior to infarction. A xylocaine infusion of 2 mg./min. was maintained for 90 minutes post-infarction. EKG monitoring was maintained throughout the experiment. Short bursts of ventricular ectopy were common following embolization and were treated with 50 to 100 mg. boluses of xylocaine. Precordial ST segment elevation was noted in all animals. When the animals appeared electrically stable, the cutdown was closed, 100 mg of xylocaine infiltrated subcutaneously around the wound, 200 mg of xylocaine administered intramuscularly and they were allowed to recover in their cages. Overall mortality secondary to ventricular arrhythmias was 20%.



Twenty-four hours following infarction the conscious animal received 10 mCi of  $^{99m}\text{Tc-PYP}$  intravenously. An hour later 0.5 mCi of  $^{43}\text{K}$  was also given intravenously. One minute after the  $^{43}\text{K}$  injection, the dogs were anesthetized, endotracheal intubation performed, and respiration maintained on a Harvard respirator. A lateral thoracotomy was performed at the level of the left fourth intercostal space to obtain adequate exposure of the beating heart. The left atrial appendage was then cannulated and approximately 4.4-6 million  $15\pm 5$  micron diameter microspheres were administered. The microspheres had been under constant agitation in an ultrasonic bath for at least 15 minutes before injection and also had been vigorously shaken manually; these two procedures retard settling and clumping of the microspheres. This large number of microspheres was employed to improve overall counting statistics and has been shown not to alter coronary blood flow significantly (39).

Two minutes following microsphere injection the heart was removed and washed. In all instances the site of plug embolization could be identified and epicardial demarcation of the site of infarction was evident. The atria, right ventricle, and interventricular septum were dissected free from the left ventricle. Samples were obtained from the mid-left anterior descending distribution of the left ventricle (infarct zone) and from the normal circumflex distribution of the lateral wall. Approximately 12-16 two gram myocardial samples were obtained from each animal. The topography



of each sample in relation to the infarct zone and coronary anatomy was recorded. Samples were trimmed of epicardial fat and blood vessels and divided into approximately equal one gram endocardial and epicardial halves.

Samples then were counted in a well-type scintillation counter. Utilizing differential spectrometry  $^{43}\text{K}$  activity was counted at a window from 560-660 KeV,  $^{51}\text{Cr}$  microsphere activity at a window of 300-340 KeV and  $^{99\text{m}}\text{Tc-PYP}$  at a window of 100-140 KeV. After physical decay of a major portion of the overlapping higher energy  $^{43}\text{K}$ , a more optimal condition existed for counting  $^{51}\text{Cr}$ . Therefore,  $^{51}\text{Cr}$  and  $^{43}\text{K}$  activity was recounted approximately four days after study.

By counting a  $^{43}\text{K}$  standard in the  $^{43}\text{K}$ ,  $^{51}\text{Cr}$ , and  $^{99\text{m}}\text{Tc}$  windows and a  $^{51}\text{Cr}$  standard in the  $^{51}\text{Cr}$  and  $^{99\text{m}}\text{Tc}$  windows, ratios were obtained for correcting the higher activity  $^{43}\text{K}$  and  $^{51}\text{Cr}$  in the  $^{99\text{m}}\text{Tc}$  window and for correcting the  $^{43}\text{K}$  activity present in the  $^{51}\text{Cr}$  window. For example,  $^{51}\text{Cr}$  counts per minute (cpm) is equal to the raw counts in the  $^{51}\text{Cr}$  window minus the counts there due to scatter from the higher energy  $^{43}\text{K}$ . This number is obtained by multiplying the  $^{43}\text{K}$  ratio times the raw counts in the  $^{43}\text{K}$  window. Thus, the calculations are represented by using the following abbreviations:

$^{43}\text{K}$  STD in  $^{43}\text{K}$  window = A

$^{43}\text{K}$  STD in  $^{51}\text{Cr}$  window = B

$^{43}\text{K}$  STD in  $^{99\text{m}}\text{Tc}$  window = C

$^{51}\text{Cr}$  STD in  $^{51}\text{Cr}$  window = D





$^{51}\text{Cr}$  STD in  $^{99\text{m}}\text{Tc}$  window=E

Raw Counts in  $^{43}\text{K}$  window= $^{43}\text{K}$

Raw Counts in  $^{51}\text{Cr}$  window= $^{51}\text{Cr}$

Raw Counts in  $^{99\text{m}}\text{Tc}$  window= $^{99\text{m}}\text{Tc}$

Calculation 1. Corrected  $^{51}\text{Cr}$  cpm=  $^{51}\text{Cr}$  minus  $(\frac{B}{A} \times ^{43}\text{K})$

Similarly, the  $^{99\text{m}}\text{Tc}$ -PYP counts per minute is equal to the raw counts in the  $^{99\text{m}}\text{Tc}$ -PYP window minus the counts due to scatter from higher energy  $^{43}\text{K}$  and  $^{51}\text{Cr}$ . Thus, corrected  $^{99\text{m}}\text{Tc}$ -PYP cpm equals the following equation:

Calculation 2. Corrected  $^{99\text{m}}\text{Tc}$  cpm=  $^{99\text{m}}\text{Tc}$  minus

$(\frac{C}{A} \times ^{43}\text{K} \text{ plus } \frac{E}{D} \times \text{Corrected } ^{51}\text{Cr cpm})$

Sample activity was expressed as an activity ratio between that of the sample and the mean value of the 6-8 normal samples obtained in each animal.

Four sham infarcted animals served as controls for these studies. In these animals following intravenous administration of the soluble radioactive tracers and left-atrial microsphere injection, the heart was removed and samples obtained and analyzed as outlined previously.



## RESULTS

In all 12 animals studied, significant abnormalities existed in the myocardial uptake of  $^{43}\text{K}$  and  $^{99\text{m}}\text{Tc-PYP}$  in the infarct zone. Infarct to normal radioactivity ratios averaged  $0.53 \pm 0.03$  for  $^{43}\text{K}$  and  $11.1 \pm 2.0$  for  $^{99\text{m}}\text{Tc-PYP}$ . In each experiment values for infarct zone radioactivity were significantly different ( $p < 0.001$ ) from those in normal zones. Similarly,  $^{51}\text{Cr}$  microsphere distributions were significantly abnormal in the infarct zone ( $p < 0.001$ ) with an average infarct to normal radioactivity ratio of  $0.55 \pm 0.03$ . The data from a typical experiment are shown in Figure 1. In sham infarct control animals the standard deviation of the mean and standard error for  $^{43}\text{K}$  samples averaged 6% and 3% respectively, for  $^{99\text{m}}\text{Tc-PYP}$  4% and 2% respectively, and for  $^{51}\text{Cr}$  microspheres 6% and 3% respectively.

When the relationships between  $^{99\text{m}}\text{Tc-PYP}$  and  $^{43}\text{K}$  uptake were compared in 91 samples, no simple linear relationship existed.  $^{99\text{m}}\text{Tc-PYP}$  uptake was maximal in regions associated with  $^{43}\text{K}$  uptake of approximately 0.4 of normal. A positive relationship existed in samples in which  $^{43}\text{K}$  uptake was less than 0.4 of normal, such that as  $^{43}\text{K}$  uptake increased,  $^{99\text{m}}\text{Tc-PYP}$  uptake similarly increased ( $r = 0.73$ ). In infarct regions with  $^{43}\text{K}$  uptake greater than 0.4 of normal, a negative linear relationship existed, such that as  $^{43}\text{K}$  uptake increased and approached normal,  $^{99\text{m}}\text{Tc-PYP}$  uptake fell ( $r = 0.75$ ) (Figure 2). Similar trends were apparent in com-



paring epicardial and endocardial samples as well.

Microsphere studies based upon the same samples from 12 animals demonstrated an excellent linear correlation between regional myocardial uptake of the flow related particles and ionic  $^{43}\text{K}$  (Figures 3,4,5). This relationship existed for transmural samples ( $r = 0.93$ ) as well as endocardial ( $r = 0.97$ ) and epicardial ( $r = 0.86$ ) portions. In extremely low flow regions, the radioactive cation uptake was generally greater than that of microspheres.

On the other hand, the relationship between flow-related microsphere distribution and that of  $^{99\text{m}}\text{Tc-PYP}$  was by no means linear.  $^{99\text{m}}\text{Tc-PYP}$  uptake was maximal at relative microsphere flow distributions between 0.30 and 0.40 of normal (Figure 6). At regional myocardial blood flow less than 0.40 of normal,  $^{99\text{m}}\text{Tc-PYP}$  myocardial uptake increased as flow increased; at regional myocardial blood flow rates greater than 0.4 of normal,  $^{99\text{m}}\text{Tc-PYP}$  uptake decreased as flow approached normal. However, in relatively high flow border segments (greater than 0.80 of normal) significant  $^{99\text{m}}\text{Tc-PYP}$  uptake of approximately 5-6 times normal persisted. Similar trends were noted in comparison of endocardial and epicardial samples.

Of note as well was the transmural distribution of  $^{99\text{m}}\text{Tc-PYP}$  uptake within the infarct zone (Figure 7). In low flow regions, pyrophosphate myocardial uptake was primarily epicardial, with endo/epicardial ratios of 0.4-0.5. As the regional flow profile increased toward normal, transmural



distribution became equivalent between endocardium and epicardium. In the highest flow border zones of the infarct,  $^{99m}\text{Tc}$ -PYP uptake was primarily endocardial with endo-epicardial ratios of 3-3.5.





## DISCUSSION

Radionuclide imaging techniques represent sensitive new tools in the clinical armamentarium because they are able to describe in a noninvasive manner physiologic and pathologic phenomenon not easily obtainable by other methods. If they are to be useful, not only to detect myocardial ischemia and infarction, but also to quantify their respective size, however, then the factors which govern their individual myocardial uptake must be clearly understood. Such insights can be gained from animal models as long as one recognizes that direct comparison to man is difficult because species variation in coronary anatomy and collateral pathways may be significant.

Initially this study had two objectives: 1) to examine the relationship between regional myocardial blood flow and the myocardial uptake of the radioactive tracers  $^{43}\text{K}$  and  $^{99\text{m}}\text{Tc-PYP}$ . 2) To examine the interrelationships between myocardial uptake of  $^{43}\text{K}$  and that of  $^{99\text{m}}\text{Tc-PYP}$ . These goals were realized. In addition, other interesting observations about the accumulation of  $^{99\text{m}}\text{Tc-PYP}$  became apparent.

First of all, there was an excellent correlation between myocardial uptake of  $^{43}\text{K}$  and regional myocardial blood flow as estimated by the radioactive microsphere technique. This high correlation existed in both endocardial and epicardial samples as well as across the entire wall thickness. These studies in a closed-chest 24 hour infarct



preparation agree closely with data obtained in more acute open chest canine preparations by Prokop et al. (32) , Becker et al. (47), and Strauss et al. (48). In this study, as in the others mentioned, radioactive cation uptake was somewhat greater than that of microspheres in very low flow regions.

In comparison, the relationship of  $^{99m}\text{Tc}$ -PYP to regional myocardial blood flow is much more complex. As regional myocardial blood flow increases from the central infarct zone to the periphery,  $^{99m}\text{Tc}$ -PYP accumulation at first increases linearly with blood flow; it then reaches a maximum at a blood flow reduction of approximately 0.4 of normal; finally, it decreases linearly as blood flow continues to increase and approach normal. Although no histologic sections were taken to examine the extent of myocardial necrosis, it appears that  $^{99m}\text{Tc}$ -PYP uptake in the infarct is governed by at least two factors: 1) regional flow to the involved area which allows delivery of the radioactive tracer, 2) extraction of the tracer which is dependent upon myocardial necrosis or ischemic injury.

The transmural distribution of  $^{99m}\text{Tc}$ -PYP within the infarct zone also illustrates the role of regional blood flow in determining radionuclide uptake. In regions of lowest flow within the center of the infarct,  $^{99m}\text{Tc}$ -PYP uptake is predominantly epicardial, with endo-eipcardial ratios of 0.4-0.5. This occurs despite the fact that the more intense local region of necrosis would involve the endocardial sur-



face of the infarcted segment. On the other hand, in higher flow regions, uptake becomes primarily endocardial. These observations of pyrophosphate uptake stand in direct contrast to those recently obtained with radioactively labelled myosin specific antibodies (23,24). With this radioactive tracer, uptake in the central infarction zone is primarily endocardial, and maximal uptake occurs in the lowest flow regions. Thus, it again becomes apparent that  $^{99m}\text{Tc}$ -PYP myocardial uptake is dependent both on flow and on some alteration of the myocardial cell.

Furthermore, in analysis of the microsphere data one notes significant myocardial  $^{99m}\text{Tc}$ -PYP uptake (approximately 5.3 times normal) in regions where flow is minimally if at all reduced (greater than 0.80 of normal). This implies either uptake in ischemic but not irreversibly damaged cells or uptake by a small population of infarcted myocardial cells interspersed with a normal population within the border zone. Discrimination between these alternative possibilities will require the use of techniques such as autoradiography. A possible clinical correlate of this phenomenon might be the finding of positive myocardial images of abnormal pyrophosphate uptake in patients with unstable angina who demonstrate neither serum enzyme nor electrocardiographic evidence of infarction (17).

Given the excellent correlation between regional myocardial blood flow distribution and  $^{43}\text{K}$  accumulation, one would expect the bimodal relationship that is obtained between



$^{43}\text{K}$  and  $^{99\text{m}}\text{Tc-PYP}$  to be very similar to that between  $^{51}\text{Cr}$  and  $^{99\text{m}}\text{Tc-PYP}$ . This data concerning the relationships between pyrophosphate uptake and other radioactive cationic myocardial distributions are in general agreement with other recent preliminary reports utilizing either radioactive potassium (83), Cesium (77), and Thallium (82). Furthermore, the correlative data with both  $^{43}\text{K}$  and microspheres indicate that if flow is significantly reduced, then a falloff in maximal pyrophosphate uptake would be expected. An in vivo imaging concomitant of these observations would be the "doughnut" appearance of reduced central  $^{99\text{m}}\text{Tc-PYP}$  accumulation noted in images of canine and human infarction involving the anterior wall of the left ventricle (81).

Although the biochemical mechanisms governing  $^{99\text{m}}\text{Tc-PYP}$  uptake have not yet been resolved, some extrapolations can be made from these data, obtained at the tissue level, to the external detection of myocardial radionuclide distributions in the patient with myocardial infarction. By using computer generated isocount contour maps, one would expect radioactive cation distributions to correspond well with flow-related parameters of infarcted and ischemic myocardium. On the other hand  $^{99\text{m}}\text{Tc-PYP}$  uptake might well be lower in central infarction zones and excessively high in the perimeter or margin zone, such that overall infarct size might be overestimated. If "cold and hot spot" tracers were used together, subtraction of the isocount distribution of one radionuclide from that of the other might allow definition of a region of





"mismatch" or "nonalignment." This zone would correspond to an ischemic periinfarction area. In addition, sequential hot spot imaging following an interim increase in regional myocardial blood flow could lead to increased  $^{99m}\text{Tc}$ -PYP uptake and apparent worsening on scan although the situation in fact, would be improving. Recent reports emphasize the additional information gained by dual radionuclide imaging (15,25,26,27,82,83).

In summary, in the twenty-four hour old canine infarct model, dual radionuclide myocardial distribution studies reveal a direct correlation between radioactive monovalent cation uptake, as measured by  $^{43}\text{K}$ , and regional myocardial blood flow. On the other hand, infarct pyrophosphate uptake is partially dependent on delivery of the radioactive tracer to the infarct zone yielding maximal uptake at 0.3-0.4 normal flow, with epicardial uptake predominating in low flow zones. These data help to define the pathophysiologic correlates of dual radionuclide tracer uptake in the myocardium.

Vincent C. DiCola



## SUMMARY

The dual radionuclide myocardial distributions of the imaging agents potassium-43 ( $^{43}\text{K}$ ) and technetium-99m stannous pyrophosphate ( $^{99\text{m}}\text{Tc-PYP}$ ) were studied 24 hours following closed-chest canine infarction. In multiple myocardial biopsies from 12 dogs, tissue levels of both radionuclides were compared and related to estimates of regional myocardial blood flow (RMBF) as measured by the distribution of radioactive microspheres.

There was an excellent correlation between myocardial  $^{43}\text{K}$  uptake in ischemic and infarcted zones and microsphere estimates of RMBF. The relationship of  $^{99\text{m}}\text{Tc-PYP}$  uptake to microsphere estimates of RMBF was more complex, however, and demonstrated maximal  $^{99\text{m}}\text{Tc-PYP}$  uptake at flows of 0.3 to 0.4 of normal. At lower flows  $^{99\text{m}}\text{Tc-PYP}$  uptake increased with increasing tissue perfusion. At higher flows  $^{99\text{m}}\text{Tc-PYP}$  uptake decreased with increasing tissue perfusion. A similar relationship was noted between the distributions of  $^{99\text{m}}\text{Tc-PYP}$  and  $^{43}\text{K}$ . In the low flow regions  $^{99\text{m}}\text{Tc-PYP}$  uptake was primarily epicardial; in the higher flow periphery of the infarct endocardial uptake predominated and significant endocardial  $^{99\text{m}}\text{Tc-PYP}$  uptake occurred despite near normal RMBF.

Thus, while there is a direct correlation between cationic  $^{43}\text{K}$  myocardial uptake and RMBF, no such direct relationship



### SUMMARY (Continued)

exists for  $^{99m}\text{Tc}$ -PYP since uptake of this tracer is dependent both on the magnitude of necrosis and on flow-related delivery of the tracer to the infarct zone. The implications of this study for dual radionuclide imaging of infarction are discussed.



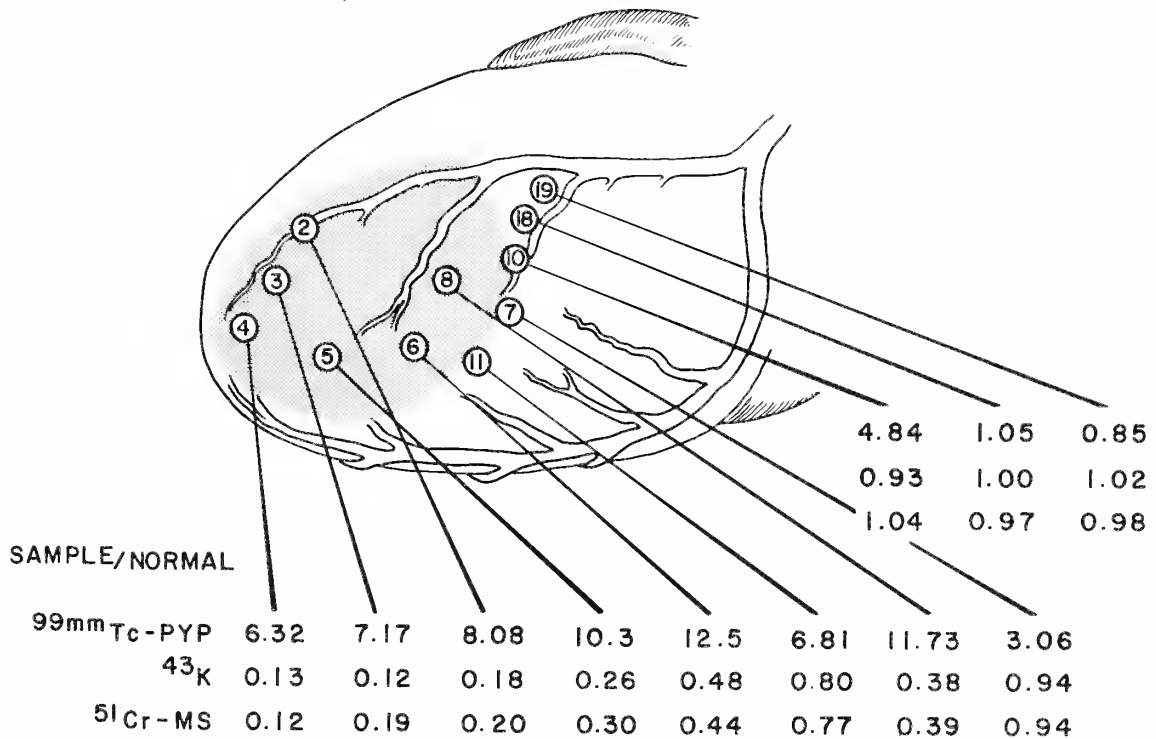


FIGURE 1. Diagrammatic representation of the topography of dual radionuclide distribution in an individual study. The stippled area indicates the visually appreciated zone of infarction. The plug embolus is situated in the left anterior descending coronary artery just proximal to the last large diagonal branch. The numbers in circles correspond to sample biopsy sites in the individual experiment. Sample activities for technetium-99m pyrophosphate, potassium-43 and chromium-51 microspheres are expressed as activity ratios between the infarct sample and the mean of 6-8 normal biopsies remote from the infarct. Abnormality in potassium-43 uptake parallels chromium-51 microsphere distribution. Highest technetium-99m pyrophosphate activity is noted in sample 6 which is near the margin of infarction and has only moderate reduction in potassium-43 and chromium-51 microsphere uptake. Relatively low technetium-99m pyrophosphate activity is noted in sample 4 which has the lowest potassium-43 and chromium-51 microsphere accumulation.





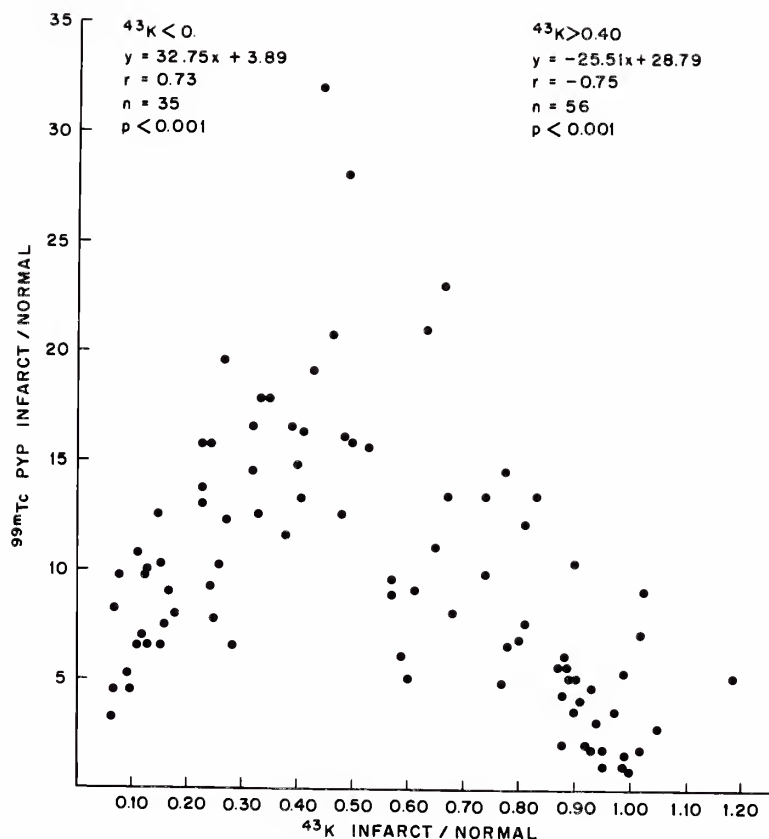


FIGURE 2. Relationship between myocardial potassium-43 and technetium-99m pyrophosphate activities in 91 samples from 12 dogs. Note that maximum technetium-99m pyrophosphate activity occurs at potassium-43 levels between 0.30 and 0.40 of normal. Two significant linear relationships are evident. At potassium-43 levels below 0.4 of normal, technetium-99m pyrophosphate levels increase as potassium-43 activity increases. At potassium-43 levels greater than 0.40 of normal, technetium-99m pyrophosphate decreases as potassium-43 increases toward normal.

1920年12月  
1921年1月  
1921年2月

1921年3月  
1921年4月  
1921年5月

RELATIONSHIP OF TRANSMURAL  $^{43}\text{K}$   
AND  $^{51}\text{Cr}$  MICROSPHERES

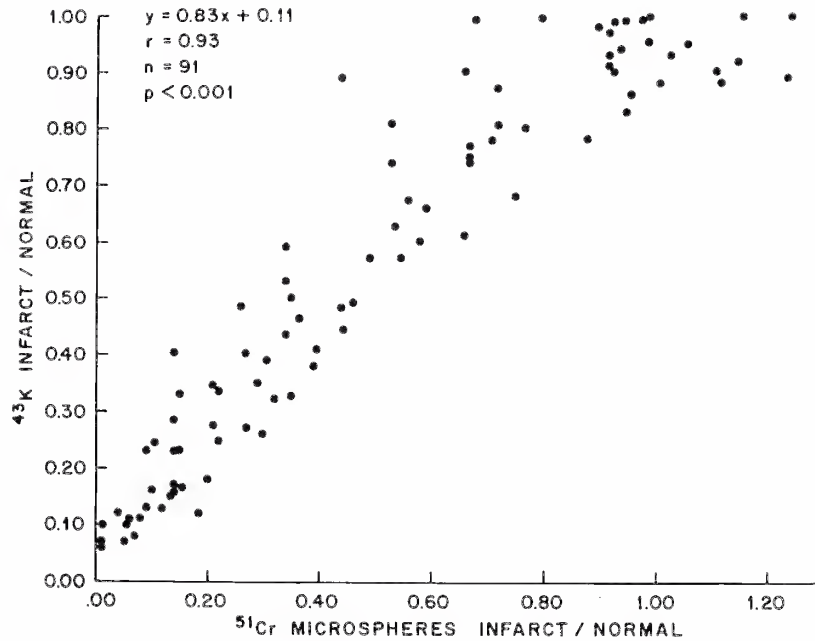


FIGURE 3. Significant linear relationship is evident between potassium-43 uptake and chromium-51 microsphere distributions in transmural samples.



RELATIONSHIP OF  $^{43}\text{K}$  AND  
 $^{51}\text{Cr}$  MICROSPHERE ENDOCARDIAL DISTRIBUTIONS

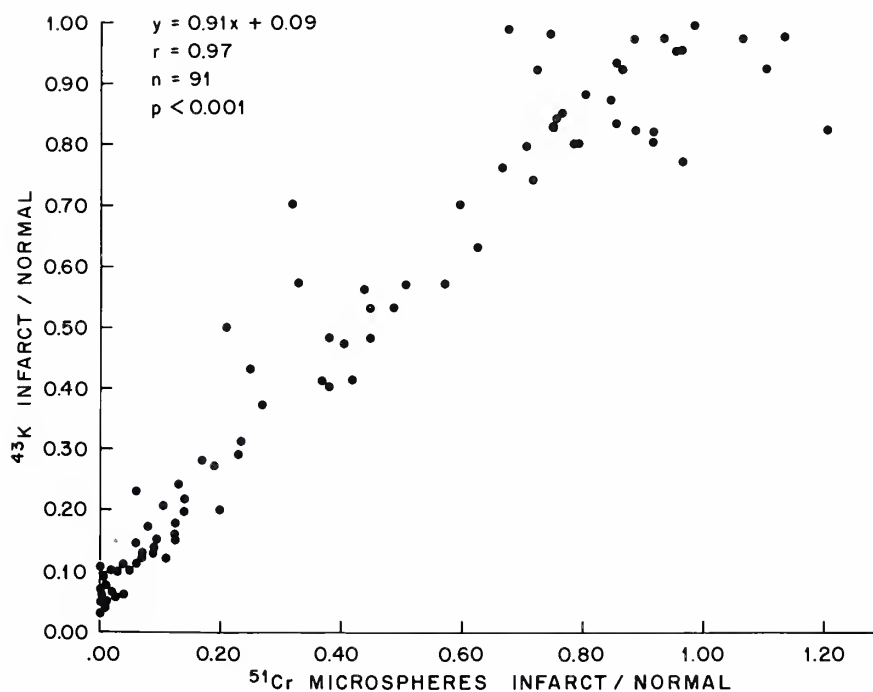


FIGURE 4. Significant linear relationship is evident between potassium-43 uptake and chromium-51 microsphere distributions in endocardial samples.



# RELATIONSHIP OF $^{43}\text{K}$ AND $^{51}\text{Cr}$ MICROSPHERE EPICARDIAL DISTRIBUTIONS

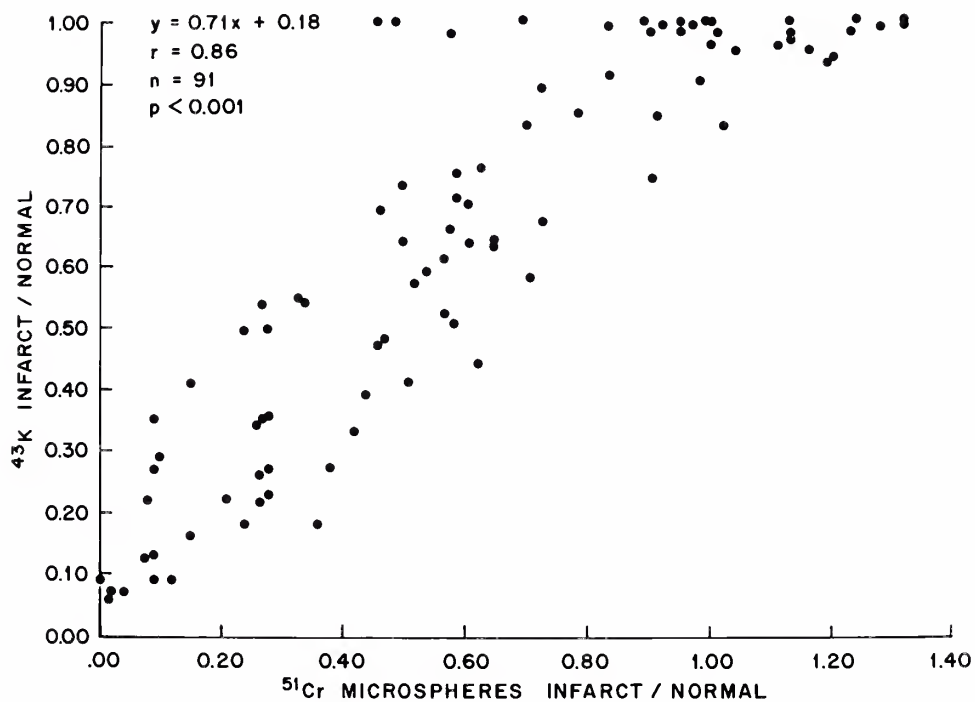


FIGURE 5. Significant linear relationship is evident between potassium-43 uptake and chromium-51 microsphere distributions in epicardial samples.





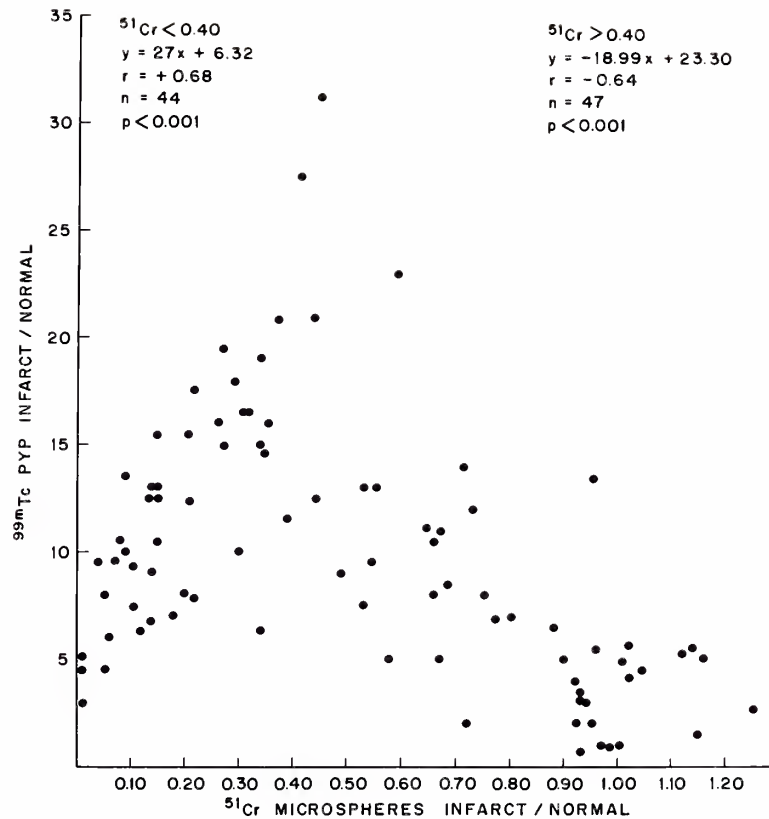


FIGURE 6. Relationships between myocardial technetium-99m pyrophosphate and chromium-51 microsphere distributions in the transmural sample. Note the similarity in distributions to the relationships between potassium-43 and technetium-99m pyrophosphate; uptake is again maximal at relative flows of between 0.30 - 0.40 of normal. Note the frequent finding of abnormal technetium-99m pyrophosphate uptake in relatively high flow border zones.



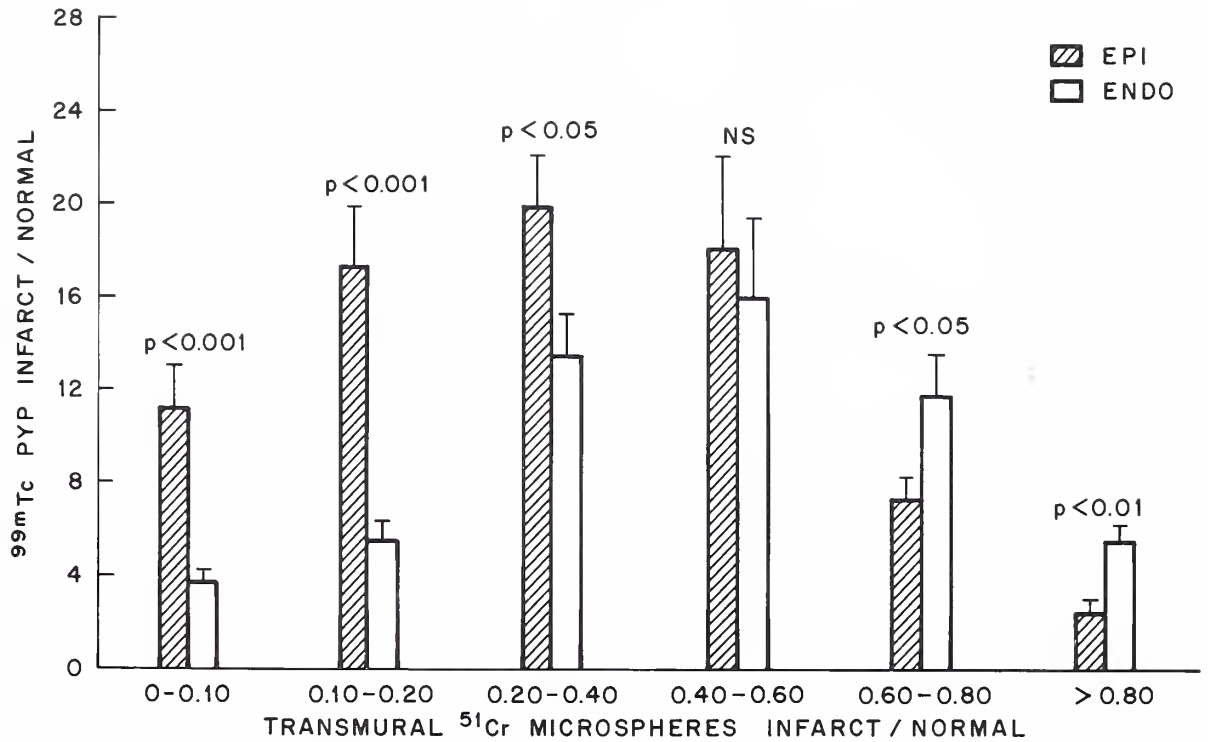


FIGURE 7. Endocardial and epicardial distributions of technetium-99m pyrophosphate in relation to chromium-51 microsphere estimates of relative blood flow in 91 samples from 12 dogs. Epicardial activity is shown by the cross-hatched bars, endocardial activity by the open bars. SEM is given for each group. P values refer to significant differences between endo- and epicardial portions within each flow zone. Note that technetium-99m pyrophosphate uptake is primarily epicardial in low flow zones, with a gradual transition as flow increases toward normal.



## BIBLIOGRAPHY

1. Kjekshus JK, Sobel BE: Depressed Myocardial Creatine Phosphokinase Activity Following Experimental Myocardial Infarction. *Circulation Res* 27:403, 1970.
2. Shell WE, Kjekshus JK, Sobel BE: Quantitative Assessment of the Extent of Myocardial Infarction in the Conscious Dog by Means of Analysis of Serial Changes in Serum Creatine Phosphokinase Activity. *J Clin Invest* 50:2614, 1971.
3. Sobel BE, Bresnahan GF, Shell WF, Yoder RD: Estimation of Infarct Size in Man and its Relation to Prognosis. *Circulation* 46:640, 1972.
4. Moroko PR, Kjekshus JK, Sobel BE, Watanabe T, Covell JW, Ross J Jr, Braunwald E: Factors Influencing Infarct Size following Experimental Coronary Artery Occlusions. *Circulation* 43:67, 1971.
5. Moroko PR, Libby P, Covell JW, Sobel BE, Ross J Jr, Braunwald E: Precordial S-T Segment Elevation Mapping: An Atraumatic Method for Assessing Alterations in the Extent of Myocardial Ischemic Injury: The Effects of Pharmacologic and Hemodynamic Interventions. *Am J Cardiol* 29:223, 1972.
6. Moroko PR, Braunwald E: Modification of Myocardial Infarction Size after Coronary Occlusion. *Ann Int Med* 79:720, 1973.
7. Zaret BL, Strauss HW, Martin ND, Flamm MD: Noninvasive Regional Myocardial Perfusion with Radioactive Potassium: Study of Patients at Rest, with Exercise and During Angina Pectoris. *NEJM* 288:809, 1973.
8. Botti RE, MacIntyre WS, Pritchard WH: Identification of Ischemic Area of Left Ventricle by Visualization of <sup>43</sup>K Myocardial Deposition. *Circulation* 47:486, 1973.
9. Zaret BL, Vlay SC, Freedman GS, Wolfson S, Cohen LS: Quantitative Relationships between Potassium-43 Imaging and Left Ventricular Cineangiography following Myocardial Infarction in Man. *Circulation* 52:1076, 1975.
10. Martin ND, Zaret BL, McGowan RL, Wells HP, Flamm MD: Rubidium-81, A New Myocardial Scanning Agent: Noninvasive Regional Myocardial Perfusion Scans at Rest and Exercise and Comparison with Potassium-43. *Radiology* 111:651, 1974.

1. The first part of the paper discusses the importance of the study of the history of the United States.

2. The second part of the paper discusses the importance of the study of the history of the United States.

3. The third part of the paper discusses the importance of the study of the history of the United States.

4. The fourth part of the paper discusses the importance of the study of the history of the United States.

11. Shames DH, Botvinick EH, Gershengorn K, Parmely WW: Advantages of Stress Myocardial Imaging over Stress Electrocardiography. Circulation Suppl 2 to Vol 52: 239, 1975 (Abst).
12. Ronhilt DW, Adolph RJ, Sodd VJ, Levenson NI, August LS, Nishiyama H, Berke RA: Cesium-129 Myocardial Scintigraphy to Detect Myocardial Infarction. Circulation 48:1242, 1973.
13. Gustin B, Ronhilt D, Adolph R, Ashard A, Levenson N, Sodd V, August L, Kahn J: Cesium-129 Myocardial Scintigraphy to Quantify and Localize Acute Myocardial Infarction. Circulation Suppl 2 to Vol 52:53, 1975 (Abst).
14. Lebowitz E, Greene MW, Fairchild R, Bradley-Moore PR, Atkins HL, Ansari AN, Richards P, Belgrave E: Thallium-201 for Medical Use. J Nucl Med 16:151, 1975.
15. Parkey RW, Bonte FJ, Stokely EM, Lewis SE, Buja LM, Willerson JT: Acute Myocardial Infarction Imaged with Both Technetium-99m Stannous Pyrophosphate and Thallium-201: A Clinical Evaluation. Circulation Suppl 2 to Vol 52:71, 1975 (Abst).
16. Bonte FJ, Parkey RW, Graham KD, Moore J, Stokely EM: A New Method of Radionuclide Imaging of Myocardial Infarcts. Radiology 110:473, 1974.
17. Willerson JT, Parkey RW, Bonte FJ, Meyer SL, Atkins JM, Stokely EM: Technetium Stannous Pyrophosphate Myocardial Scintigrams in Patients with Chest Pain of Varying Etiology. Circulation 51:1046, 1975.
18. Holman BL, Lesch M, Zwelman FG, Temte J, Lown B, Godin R: Detection and Sizing of Acute Myocardial Infarcts with  $^{99m}\text{Tc}$  (SN) Tetracycline. NEJM 291:159, 1974.
19. Fink/Bennett D, Dworkin HJ, Lee YH: Myocardial Imaging of the Acute Infarct. Radiology 113:449, 1974.
20. Strauss HW, Rouleau J, Rowman D, Pitt B: Detection of Acute Myocardial Infarction in Patients with Technetium 99m Glucoheptonate. (Abstract) Am J Cardiol 35:171, 1975.
21. Rossman DJ, Rouleau J, Strauss HW, Pitt B: Tc-99m-Glucoheptonate for the Identification of Acute Myocardial Infarction. (Abstract) J Nucl Med 16:563, 1975.
22. Lesch M, Tanaka T, Holman BL: Comparative Accuracy of  $^{99m}\text{Tc}$  Pyrophosphate,  $^{99m}\text{Tc}$ -Tetracycline, and  $^{99m}\text{Tc}$ -Glucoheptonate for the Scintigraphic Diagnosis of Acute Myocardial Infarction. Circulation Suppl 2 to Vol 52:53, 1975 (Abst).

II. 25000  
Advantage  
Bisecting  
1900

III. 25000  
Advantage  
Bisecting  
1900

IV. 25000  
Advantage  
Bisecting  
1900

V. 25000  
Advantage  
Bisecting  
1900

VI. 25000  
Advantage  
Bisecting  
1900

VII. 25000  
Advantage  
Bisecting  
1900

VIII. 25000  
Advantage  
Bisecting  
1900

IX. 25000  
Advantage  
Bisecting  
1900

X. 25000  
Advantage  
Bisecting  
1900

XI. 25000  
Advantage  
Bisecting  
1900

XII. 25000  
Advantage  
Bisecting  
1900

XIII. 25000  
Advantage  
Bisecting  
1900



23. Khaw BA, Beller GA, Haber E, Smith TW: Localization and Sizing of Myocardial Infarcts Employing Radioactively Labeled Myosin Specific Antibody. Clin Res 23:381A, 1975 (Abst).
24. Khaw BA, Beller GA, Haber E, Smith TW: Comparison of Radiolabelled Myosin Specific Antibody and Technetium-99m Stannous Pyrophosphate ( $^{99m}\text{Tc}$  PYP) for Localization of Myocardial Infarcts. Circulation Suppl 2 to Vol 52:52, 1975 (Abst).
25. Henning H, Schelbert H, Rigletti A, Ashburn W, O'Rourke R: Comparison between Tc-99m-Pyrophosphate (PYP) and Thallium-201 (Tl) for Diagnosing Acute Myocardial Infarction. Circulation Suppl 2 to Vol 52:194, 1975 (Abst).
26. Nishimura A, Gorten RJ, Kim YI, Williams JF Jr: Dual Radionuclide Myocardial Scanning for Diagnosis and Location of Acute Myocardial Infarcts. Circulation Suppl 2 to Vol 52:223, 1975 (Abst).
27. Bing RJ, Rickart A, Hellberg K: Techniques to Measure Coronary Blood Flow in Man. Am J Cardiol 29:75, 1972.
28. Gould KL, Lipscomb K, Hamilton GW: Physiologic Basis for Assessing Critical Coronary Stenosis. Instantaneous Flow Response and Regional Distribution during Coronary Hyperemia as Measures of Coronary Flow Reserve. Am J Cardiol 33:87, 1974.
29. Becker LC, Pitt B: Collateral Blood Flow in Conscious Dogs with Chronic Coronary Artery Occlusion. Am J Physiol 221:1507, 1971.
30. Becker LC, Fortuin NJ, Pitt B: Effect of Ischemia and Antianginal Drugs on the Distribution of Radioactive Microspheres in the Canine Left Ventricle. Circulation Res 28:263, 1971.
31. Becker LC, Ferreira R, Thomas M: Effect of Propranolol and Isoprenaline on Regional Left Ventricular Blood Flow in Experimental Myocardial Ischemia. Cardiovascular Res 9:178, 1975.
32. Prokop EK, Strauss HW, Shaw J, Pitt B, Wagner H N Jr: Comparison of Regional Myocardial Perfusion Determined by Ionic Potassium-43 to that Determined by Microspheres. Circulation 50:978, 1974.
33. Eckenhoff JE, Hafkenschield JH, Harmel MH, Goodade WT, Lubin M, Bing RJ, Kety SS: Measurement of Coronary Blood Flow by the Nitrous Oxide Method. Am J Physiol 152:356, 1948.



34. Salisbury PF, Cross CE, Oblath RW, Ruben PA: Local Circulation in Heart Muscle Studied with Na<sup>24</sup> Clearance Method. J Appl Physiol 17:475, 1962.
35. Bassingthwaight JB, Strandell T, Donald DE: Estimation of Coronary Blood Flow by Washout of Diffusible Indicators. Circulation Res 23:259, 1968.
36. Love WD: Isotope Clearance and Myocardial Blood Flow. Am Heart J 67:579, 1964.
37. Rudolph AM, Heymann MA: The Circulation of the Fetus in Utero: Methods for Studying Distribution of Blood Flow, Cardiac Output and Organ Blood Flow. Circulation Res 21:163, 1967.
38. Domenech RJ, Hoffman JIE, Noble MIM, Saunders KB, Henson JR, Subijanto S: Total and Regional Coronary Blood Flow Measured by Radioactive Microspheres in Conscious and Anesthetized Dogs. Circulation Res 25:581, 1969.
39. Fortuin NJ, Kaihara S, Becker LC, Pitt B: Regional Myocardial Blood Flow in the Dog Studied with Radioactive Microspheres. Cardiovascular Res 5:331, 1971.
40. Cutarelli R, Levy MN: Intraventricular Pressure and the Distribution of Coronary Blood Flow. Circulation Res 12:322, 1963.
41. Moir TW, DeBra DW: Effect of Left Ventricular Hypertension, Ischemia and Vasoactive Drugs on the Myocardial Distribution of Coronary Flow. Circulation Res 21:65, 1967.
42. Buckberg GB, Luck JC, Payne DB, Hoffman JIE, Archie JP, Fixler DE: Some Sources of Error in Measuring Regional Blood Flow with Radioactive Microspheres. J Appl Physiol 31:598, 1971.
43. Buckberg GD, Fixler DE, Archie JP, Hoffman JIE: Experimental Subendocardial Ischemia in Dogs with Normal Coronary Arteries. Circulation Res 30:67, 1972.
44. Domenech RJ: Total and Regional Coronary Blood Flow During Acute Coronary Occlusion in Anesthetized and Conscious Dogs. Cardiovascular Res 8:415, 1974.
45. Becker LC, Ferreira R, Thomas M: Mapping of Left Ventricular Blood Flow with Radioactive Microspheres in Experimental Coronary Artery Occlusion. Cardiovascular Res 7:391, 1973.
46. Moir TW: Subendocardial Distribution of Coronary Blood Flow and the Effect of Antianginal Drugs. Circulation Res 30:621, 1972.



- 86
47. Becker LC, Ferreira R, Thomas M: Comparison of <sup>86</sup>Rb and Microsphere Estimates of Left Ventricular Blood Flow Distribution. J Nucl Med 15:969, 1974.
  48. Strauss HW, Harrison K, Langan JK, Lebowitz E, Pitt B: Thallium-201 for Myocardial Imaging: Relation of Thallium-201 to Regional Myocardial Perfusion. Circulation 51:641, 1975.
  49. Parker JO, Chiong MA, West RO, Case RB: The Effect of Ischemia and Alterations of Heart Rate on Myocardial Potassium Balance in Man. Circulation 42:205, 1970.
  50. Noonan TR, Fenn WO, Haege L: The Distribution of Injected Radioactive Potassium in Rats. Am J Physiol 132:474, 1941.
  51. Love WD, Romney RB, Burch GE: A Comparison of the Distribution of Potassium and Exchangeable Rubidium in the Organs of the Dog, Using Rubidium-86. Circulation Res 2:112, 1954.
  52. Conn HL, Robertson JS: Kinetics of Potassium Transfer in the Left Ventricle of the Intact Dog. Am J Physiol 181:319, 1955.
  53. Sapirstein LA: Regional Blood Flow by Fractional Distribution of Indicators. Am J Physiol 193:161, 1958.
  54. Donato L, Bartolomei G, Giordani R: Evaluation of Myocardial Blood Perfusion in Man with Radioactive Potassium or Rubidium and Precordial Counting. Circulation 29:195, 1964.
  55. Love WD, Smith RO, Mitchell LM, Pulley PE: Locating Areas of Reduced Coronary Blood Flow by External Measurement of Myocardial Potassium-42 Clearance. Circulation Suppl 3 to Vol 34:160, 1960 (Abst).
  56. Bennett KR, Smith RO, Lehan PH, Hellems HK: Correlation of Myocardial Potassium-42 Uptake with Coronary Arteriography. Radiology 102:117, 1972.
  57. Carr EA, Beierwalts WH, Wegst AV, Bartlett JD: Myocardial Scanning with Rubidium-86. J Nucl Med 3:76, 1963.
  58. Carr EA, Gleason G, Shaw J, Krantz B: The Direct Diagnosis of Myocardial Infarction by Photoscanning after Administration of Cesium 131. Am Heart J 68:627, 1964.
  59. Hurley PJ, Cooper M, Reba RC, Poggenberg KJ, Wagner HN: Potassium-43 Chloride: A New Radiopharmaceutical for Imaging the Heart. J Nucl Med 12:516, 1971.
  60. Gorten RJ: Clinical Testing of Potassium-43 Scans of the Heart. J Nucl Med 13:432, 1972 (Abst).





61. Zaret BL, Stenson RE, Martin ND, Strauss HW, Wells HP, McGowan RL, Flamm MD: Potassium-43 Myocardial Perfusion Scanning for the Noninvasive Evaluation of Patients with False-Positive Exercise Tests. *Circulation* 48:1234, 1973.
62. Bennett KR, Smith RO, Suzuki A, Lehan PH, Hellems HK: The Use of Potassium-43 Myocardial Scan in Evaluating Myocardial Revascularization. *Am J Cardiol* 31:120, 1973 (Abst).
63. Zaret BL, Martin ND, McGowan RL, Strauss HW, Wells HP, Flamm MD: Rest and Exercise Potassium-43 Myocardial Perfusion Imaging for the Noninvasive Evaluation of Aortocoronary Bypass Surgery. *Circulation* 49:688, 1974.
64. Smith RO, Bennett KR, Suzuki A, Lehan PH, Hellems HK: Myocardial Revascularization Assessed with Functional Scanning Data. *Circulation Suppl* 3 to Vol 49-50:206, 1974 (Abst).
65. Gorten RJ, Nishimura A, Williams JF: The Diagnostic Accuracy of Potassium-43 Scans in Cardiac Patients. *J Nucl Med* 15:495, 1972 (Abst).
66. Poggenberg KJ: Potassium 43: The Reactor Production, Physical Properties and Potential Availability of a Useful Radioisotope. *J Nucl Med* 12:457, 1971 (Abst).
67. Smith RO, Lehan PH, Hellems HK, Poggenberg KJ: Scatter Problem when Counting the Lower Energies of Potassium-43. *J Nucl Med* 12:464, 1971 (Abst).
68. Carr EA, Beierwaltes WH, Patno ME, Bartlett JD, Wegst AV: The Detection of Experimental Myocardial Infarcts by Photoscanning. *Am Heart J* 64:650, 1962.
69. Hubner PJB: Radioisotope Detection of Experimental Myocardial Infarction using Mercury Derivatives of Fluorescein. *Cardiovascular Res* 4:509, 1970.
70. Kramer RJ, Goldstein RE, Hirshfeld JW, Roberts WC, Goldstein SE, Johnston GS: Myocardial Infarct Imaging with Gallium-67 Citrate. *J Nucl Med* 14:418, 1973.
71. Malek P, Kole J, Fastava VL, Fak F, Peleska B: Fluorescence of Tetracycline Analogues Fixed in Myocardial Infarction. *Cardiologica* 42:303, 1963.
72. Klein MS, Coleman RE, Ahmed SA, Weiss ES, Roberts R, Sobel B: <sup>99m</sup>Tc (Sn) Pyrophosphate Scintigraphy: Sensitivity, Specificity, and Mechanisms. *Circulation Suppl* 2 to Vol 52:52, 1975 (Abst).
73. Willerson JT, Parkey RW, Bonte FJ, Meyer SL, Stokely EM:





Acute Subendocardial Myocardial Infarction in Patients:  
Its Detection by Technetium  $^{99m}\text{Tc}$  Stannous Pyrophosphate  
Myocardium Scintigrams. Circulation 51:436, 1975.

74. Shames DM, Botvinick E, Lappin H, Townsend R, Tyberg J, Parmley W: Quantitation of Myocardial Infarct Size with Tc- $^{99m}$  Pyrophosphate and Correlation between Myocardial CPK Depletion and Radionuclide Uptake. J Nucl Med 16:519, 1975 (Abst).
75. Willerson JT, Parky RW, Harris RA Jr, Bonte FJ, Stokely EM, Buja LM: Sizing Acute Myocardial Infarction Utilizing Technetium Stannous Pyrophosphate Myocardial Scintigrams in Dogs and Man. Clin Res 23:214A, 1975 (Abst).
76. Botvinick E, Lappin H, Townsend R, Shames D, Tyberg J, Parmley W: Non-invasive Quantitation of Myocardial Infarction with  $^{99m}\text{Tc}$  (Sn) Pyrophosphate Correlation between Creatine Phosphokinase Depletion and Radionuclide Uptake. Am J Cardiol 35:123, 1975 (Abst).
77. Poe ND, Robinson GD, Elam DA, Battaglia DJ: A Dual Tracer Method for Evaluation of Myocardial Infarction. J Nucl Med 15:524, 1974 (Abst).
78. D'Agostino AN: An Electron Microscopic Study of Cardiac Necrosis Produced by a 9- $\alpha$ -Fluorocortisol and Sodium Phosphate. Am J Pathol 45:633, 1964.
79. D'Agostino AN, Chiga: Mitochondrial Mineralization in Human Myocardium. Am J Clin Pathol 53:820, 1970.
80. Shen AC, Jennings RB: Myocardial Calcium and Magnesium in Acute Ischemia Injury. Am J Pathol 67:417, 1972.
81. Buja LM, Parkey RW, Dees JH, Stokely EM, Harris RA Jr, Bonte FJ, Willerson JT: Morphologic Correlates of Technetium  $^{99m}$  Stannous Pyrophosphate Imaging of Acute Myocardial Infarcts in Dogs. Circulation 52:596, 1975.
82. Buja LM, Parkey RW, Stokely EM, Bonte FJ, Willerson JT: Pathophysiology of Technetium  $^{99m}$  Stannous Pyrophosphate and Thallium-201 Scintigraphy of Canine Acute Myocardial Infarcts. Circulation Suppl 2 to Vol 52:51, 1975 (Abst).
83. Poe ND, Robinson GD, Tillisch JH: Relation Between Blood Flow and Uptake of Positive Infarct Imaging Agents. J Nucl Med 16:558, 1975 (Abst).
84. Dewanjee MK, Kahn PC, Dewanjee V, Connolly RJ: Mechanism of Localization of Tc- $^{99m}$  labeled Pyrophosphate and Tetra-cycline in Infarcted Myocardium. J Nucl Med 16:525, 1975 (Abst).



85. Stevenson JS, Dunson GL: Cardiac Changes with <sup>99m</sup>Tc-tin-phosphate Radiopharmaceuticals. J Nucl Med 14:774, 1973.
86. Cohen MV, Eldh P: Experimental Myocardial Infarction in the Closed-Chest Dog: Controlled Production of Large or Small Areas of Necroses. Am Heart J 86:798, 1973.













YALE MEDICAL LIBRARY

Manuscript Theses

Unpublished theses submitted for the Master's and Doctor's degrees and deposited in the Yale Medical Library are to be used only with due regard to the rights of the authors. Bibliographical references may be noted, but passages must not be copied without permission of the authors, and without proper credit being given in subsequent written or published work.

This thesis by \_\_\_\_\_ has been  
used by the following persons, whose signatures attest their acceptance of the  
above restrictions.

---

NAME AND ADDRESS

DATE

